



## Temperature and fission rate effects on the rim structure formation in a $\text{UO}_2$ fuel with a burnup of 7.9% FIMA

M. Kinoshita <sup>a,\*</sup>, T. Kameyama <sup>a</sup>, S. Kitajima <sup>a</sup>, Hj. Matzke <sup>b</sup>

<sup>a</sup> Central Research Institute of Electric Power Industry, 2-11-1 Iwadokita Komaeshi, Tokyo 201, Japan

<sup>b</sup> European Commission, Joint Research Centre, Institute for Transuranium Elements, P.O. Box 2340, 76125 Karlsruhe, Germany

Received 23 September 1996; accepted 12 September 1997

### Abstract

A BWR design  $\text{UO}_2$  fuel irradiated to a burnup of 7.9% FIMA was selected for a careful calculational and experimental analysis because the rod experienced an unusual power history: it had two high power periods at 1.7% FIMA and between 4 and 5% FIMA causing increased fuel temperatures and thus increased gas release and damage recovery. As a consequence, two parameters generally considered to be important for grain subdivision (rim structure formation) were locally different from normal fuel, i.e. fission gas inventory and extent of radiation damage. Histories of temperature, fission rate and fission gas release were calculated at different radial positions. Microstructure observations (TEM, SEM) revealed the typical high burnup grain subdivision process (polygonization) which extended to a maximum of 1.65 mm ( $r/r_0 = 0.73$ ) from the pellet surface inwards. For this radial position, the calculations yielded a local temperature of 1200°C and predicted that more than half of the fission gas was released during the second high power period for this radial position. The results give thus information on the importance of the fission gas inventory for the burnup threshold of restructuring. © 1998 Elsevier Science B.V.

### 1. Introduction

Extension of the burnup of LWR fuel is commercially in progress. The aim is to reduce the amount of total processing turnover within the nuclear fuel cycle and to improve the costs of fuel fabrication, intermediate storage, transport and reprocessing. One of the key issues for this technological step is to understand and ultimately control the fuel micro-structural changes which start at the pellet peripheral zone, called rim-effect, evidenced by subdivision of the original grains of the sintered  $\text{UO}_2$  fuel into very small subgrains (e.g. Ref. [1]). The material properties of this restructured cylindrical shell are not known and the parameters responsible for initiation and development of the new structure are not clearly identified.

Previous findings for the initiation conditions, e.g. a burnup threshold of 70 MWd/kg U, were made by

Kameyama et al. [2], analyzing radial burnup distributions of high burnup fuels and relating them to PIE observations, especially to radial EPMA profiles of the Xe-content in the fuel. This analysis indicated that the restructuring was neither dependent on the type of the fissile atom,  $^{235}\text{U}$  or  $^{239}\text{Pu}$ , nor on the fission rate. A similar analysis was performed on a high burnup rod, AF21-2 with a well-established power history of its irradiation in the HP-1 rig in the Danish DR 3 test reactor [3] in the Risø national laboratory. This rig is similar to those used in Risø Fission Gas Release Projects [4]. This analysis confirmed that the restructuring is observed where the local temperature is below 1200°C and the burnup exceeds 70 MWd/kg U.

There are essentially two research lines which lead to progress in understanding the conditions for the formation of the rim structure. One of these consists in statistical investigations of many fuels, utilizing the growing PIE evidence on high burnup fuel and the second one consists in a careful analysis of individual fuels, or of tailor-made irradiations, in which one or more of the parameters thought to be important for the mechanism of rim structure

\* Corresponding author. Tel.: +81-3 3480 2111; fax: +81-3 3480 2493.

formation are controlled or varied in a known way as compared to normal power reactor fuel. Both lines are followed in the Institute for Transuranium Elements in Karlsruhe, the latter one in cooperation with the Central Research Institute of Electric Power Industry in Tokyo. For the former line, the work of Lassmann et al. [5] is a good example which leads to a well validated empirical description of the onset of grain subdivision, called HBS (high burnup structure) by the authors of Ref. [5]. Essentially, the description is based on assuming the coexistence of grain subdivision, formation of new pores and decrease in Xe-signal in EPMA in high burnup LWR fuels. This procedure is valuable and essential for understanding the gross restructuring in power reactor fuel as a function of burnup, but it does not yield further information on underlying mechanisms. To obtain such information is the aim of the latter line. This is achieved by a 'tailor-made' irradiation with a matrix of different burnups at different constant temperatures and with different compositions of the fuel [6] and by characterizing particular fuels selected on basis of their irradiation parameters. The tailor-made irradiation, for instance, is hoped, beyond other aims, to better define the temperature limiting grain subdivision. An example of very extended restructuring was, for example, observed in the Battelle High Burnup Programme [7] where annular pellets avoiding high central temperatures were irradiated and grain subdivision was observed both at the central hole and at the surface of the fuel pellets [8].

The objective of the present paper is the attempt to obtain information on the mechanism of grain subdivision by studying in more detail a particular fuel, i.e. the above-mentioned rod AF 21-2, by comparing more detailed refined fuel code calculations than reported in Ref. [3] with an extensive TEM/SEM investigation of the same cross section of the rod reported in a recent companion paper [9]. This particular rod was selected for this careful experimental and calculational study since it had a power history with high power periods at  $\approx 1.7\%$  FIMA and at 4–5% FIMA, and since it achieved a total burnup (7.9% FIMA) above the commonly assumed threshold for grain subdivision in LWR fuel. In contrast, typical LWR fuel experiences a steady decrease in linear power with increasing irradiation. The two high power periods of the rod AF-21-2 caused high central temperatures and were thus expected to significantly affect two parameters thought to extend important driving forces for grain subdivision, i.e. the local fission gas content in the fuel grains and the accumulated radiation damage or else the stored energy. The latter is known to be recovered upon temperature increase, the former is known to be released into grain boundary bubbles or even from the fuel at elevated temperatures. On the contrary, the concentration of non-volatile fission products, e.g. the rare earths or the rare metals and dislocation networks formed during irradiation are not affected.

There are two more ways of obtaining helpful information on the conditions leading to grain subdivision. Both

are investigated in the Institute for Transuranium Elements, but both suffer from inherent deficiencies. One consists of investigating the microstructure of Pu-rich inclusions in MOX fuel. These experience high burnup at temperature conditions which can be calculated with acceptable accuracy. However, the Pu-rich inclusions are, trivially, not  $\text{UO}_2$  fuel and they have, at constant oxygen potential, a different oxygen-to-metal ratio than  $\text{UO}_2$  which is known to affect many mass transport processes (e.g. Ref. [10]). The second way consists in introducing fission products and radiation damage into  $\text{UO}_2$  by controlled irradiation with ion beams from accelerators (e.g. Ref. [11]). With this method, a good control of temperature is possible and the fission product to be studied can be selected at will. However, not all conditions are identical with those of reactor irradiation even if ions of fission energy are used [12] and the dose rate is much higher than in reactor irradiation.

In conclusion, it was thought to be worthwhile to investigate in detail the  $\text{UO}_2$  fuel of an unusual rod like AF 21-2 to obtain information not achievable from analysis of conventional high burnup LWR fuel.

## 2. Brief summary of the experimental investigation of the analyzed cross section

In the companion paper [9], results of transmission and high resolution scanning electron microscopy of the cross section analyzed here were reported. In the rim region, the original grains of about 10  $\mu\text{m}$  diameter were subdivided into  $\approx 10^4$  subgrains of 0.15 to 0.30  $\mu\text{m}$  diameter. The spread in subgrain orientation was small ( $< 5^\circ$ ). This high burnup structure extended to a depth of 1.65 mm ( $r/r_0 = 0.73$ ). The proportion of grains showing this structure decreased from 100% at the fuel surface to very small values at depths  $> 1$  mm. The size of the subgrains was found to be largely independent of depth.

Optical microscopy (see Fig. 1) showed that the fuel indeed had experienced the calculated high temperature phase. Columnar grain growth was indicated and large metal particles were found in the pellet center, i.e. for  $r/r_0 < 0.25$  and equiaxed grain growth and fission gas decoration of grain boundaries were seen for  $r/r_0 < 0.45$ . Grain boundary porosity extended up to  $r/r_0 \approx 0.7$ .

## 3. Methods of analysis

The VIMBURN code was used to analyze the radial evolution of the local burnup. The code is composed of two sub-modules: the VIM 2 module for neutron transport and a module for the neutron reaction and decay chains [3]. VIM 2 is a code with a continuous Monte-Carlo method and a continuous energy coordinate is used for cross-sections derived from physics data of ENDF-B-IV. It is

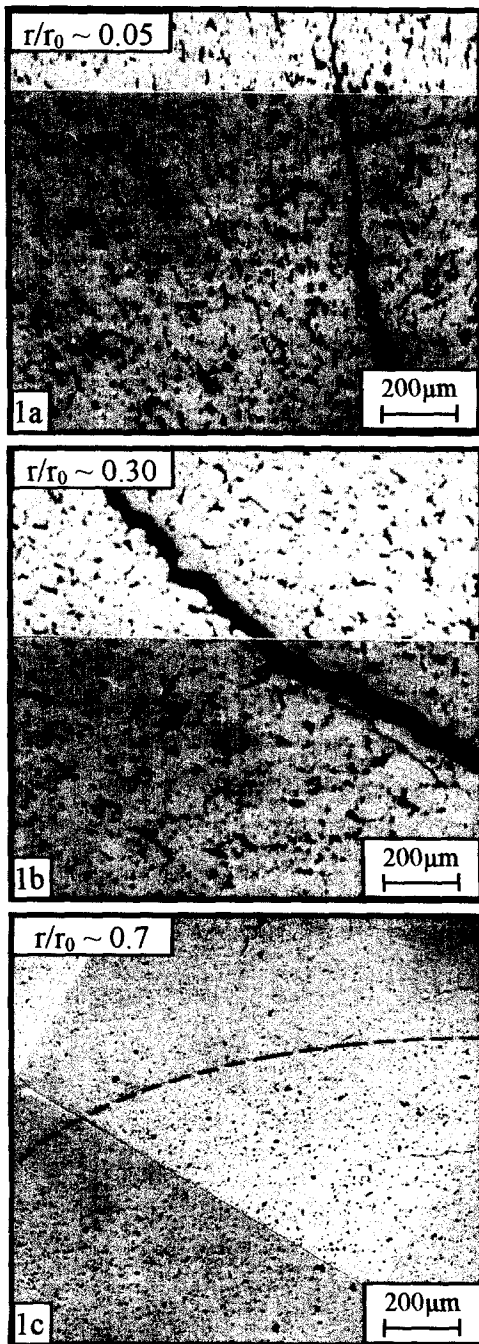


Fig. 1. Optical ceramography of the investigated fuel. (a) Central part showing columnar grain formation and large five-metal particles. (b) Zone of equiaxed grain growth. (c) Transition zone at  $r/r_0 \sim 0.7$  with increased porosity at  $r/r_0 < 0.7$ .

capable of analyzing singular resonance reactions of  $^{238}\text{U}$  at epithermal energies, which cause the neutronic rim effect in LWR fuel. The nuclides are categorized into three groups: fissile nuclides, significant absorbers such as  $^{135}\text{Xe}$  and  $^{148}\text{Sm}$  and other fission products. The module calcu-

lates depletion and generation of nuclides following the calculated rates of neutronic reactions at each burnup increment. The ORIGEN code was utilized to validate and calibrate the module.

The  $\text{UO}_2$  fuel rod analyzed in this paper was irradiated for 5.5 years in a high pressure rig of 6 cm diameter in the DR 3 reactor in Risø, Denmark. Although the neutron moderator was heavy water, the rig coolant was light water and the pressure boundary was a stainless steel tube of 1 mm thickness and 2.5 cm diameter. The VIMBURN calculation was made using this geometry and this material to estimate the variation of spatial neutron flux distribution and energy spectrum. The effect of the moderator on the radial burnup distribution was calculated in detail.

The fuel performance analysis code, EIMUS, was utilized to estimate local temperatures in the cylindrical fuel at radial positions of interest [13]. The code contains a degradation model of fuel thermal conductivity due to burnup accumulation [14]. The model accounts for two mechanisms: (1) planar porosity acting as a thermal barrier and (2) phonon scattering at dissolved fission product atoms. The former includes small cracks, separated grain boundaries and open planar porosity created after fission gas release from grain boundaries. Some of these pores are connected to the free volume of the fuel rod. This effect of connection was estimated by analysing the correlating data of fuel temperature and rod gas pressure measured at the Halden Project. The effect of solid solution of fission products, e.g. rare earths, is implemented in the model based on the thermal conductivity data of SIMFUEL [15–17]. The model is calibrated to the fuel temperature data measured at the Risø fission gas project where the burnup range was extended up to 50 MWd/kg [4,14,18].

The EIMUS code was thus improved compared to the version used for the previous analysis [3]. The rate of the decrease of fuel conductivity with burnup was assumed to be linear up to 40 MWd/kg M and constant for higher burnups. For the fission gas release, the code calculates thermal gas release with a model involving grain boundary saturation. Recoil and knock out release are also calculated. However, the code does not have a release model accounting for the restructuring by grain sub-division and polygonization, due to the lack of experimental data.

#### 4. Analysis results

The fabrication and design data of the fuel are presented in Table 1. The pellet averaged burnup of the analyzed section was estimated to be 7.9% FIMA from PIE analysis of  $^{148}\text{Nd}$ . The radial burnup profile was calculated by VIMBURN and was shown previously [3]. Due to the neutronic rim effect, the final burnup at the fuel surface is  $\approx 23\%$  FIMA, i.e. approximately three times higher than the cross section average burnup. Calculated temperatures as a function of burnup are shown in Fig. 2

Table 1  
Fabrication and irradiation data of rod AF21-2

Fuel enrichment (% $^{235}\text{U}$ )	1.5
Pellet diameter, nominal (mm)	12
Grain size ( $\mu\text{m}$ )	$\approx 5^a$
Active stack length (mm)	450
Helium filling pressure (MPa)	0.1
Coolant pressure (MPa)	7
Peak pellet average burnup (% FIMA)	7.9

<sup>a</sup>The grain size was not measured.  $5 \mu\text{m}$  is the standard value of the applied fabrication process.

for five radial positions. The temperatures at around 4% FIMA are higher than in the previous analysis [3] due to the improvement in the code in calculating the degradation of the thermal conductivity at high burnup. Grain subdivision was observed between the fuel surface ( $r/r_0 = 1$ ) and the restructuring front (or tail, depending on the point of view), i.e. at 1.65 mm depth ( $r/r_0 = 0.73$ ) [9]. The VIM-BURN analysis shows that the highest temperature was experienced between 4 and 5.2% FIMA of the local burnup at this radial location. Temperatures of up to about  $1200^\circ\text{C}$  were calculated with the EIMUS code. Following this period of increased rating and temperature, the restructuring front (or tail) experienced a 650 day long further irradiation to the final burnup of 7.2% FIMA, with the local temperature decreasing to about  $800^\circ\text{C}$ .

The calculated time history of local fission rate for again five radial locations is shown in Fig. 3. The final burnup profile, the integration of the fission rate, is in good agreement with the EPMA measurements [3] and it

shows the expected steep increase at the pellet periphery. As a result of Pu production, a steady increase of the fission rate around the pellet periphery is seen from the start of irradiation until about 1.6% FIMA of the pellet averaged burnup. At this point, the pellet surfaces reached a local burnup of 3.3% FIMA and the increase stopped because the formation and the consumption of Pu were balanced. From this time on, the fission rate at the pellet surface is approximately three times higher than the pellet average. The highest value is  $5 \times 10^{13}/\text{cm}^3 \text{ s}$  during the high power period, decreasing to  $2.5 \times 10^{13}/\text{cm}^3 \text{ s}$  during the low power period at the end of life. The fission rate in the pellet central zone decreases relatively regularly from  $1.5$  to  $0.7 \times 10^{13}/\text{cm}^3 \text{ s}$  as represented by the 1.65 mm position in Fig. 3. The calculation shows that the high fission rate is restricted to a narrow rim zone. This is due to the low enrichment of the fuel and to the extensive burning of Pu formed in the rim zone. The SEM observations [9] show that the size distributions of the restructured grains are similar and independent of the radial position between 50 and  $1570 \mu\text{m}$  though the fission rates differ by a factor of 3 to 5. This indicates that the final grain size due to the restructuring process is not significantly dependent on the fission rate within the range of  $1$  to  $5 \times 10^{13}/\text{cm}^3 \text{ s}$  (see also, however, the third paragraph of Section 5).

Based on the calculated time history of local fuel temperatures, the thermally activated fission gas release was calculated with the EIMUS code. The calculated release and the EPMA measurements of retained gas are plotted in Fig. 4. The total xenon production is also shown for comparison. Three radial zones are indicated by arrows

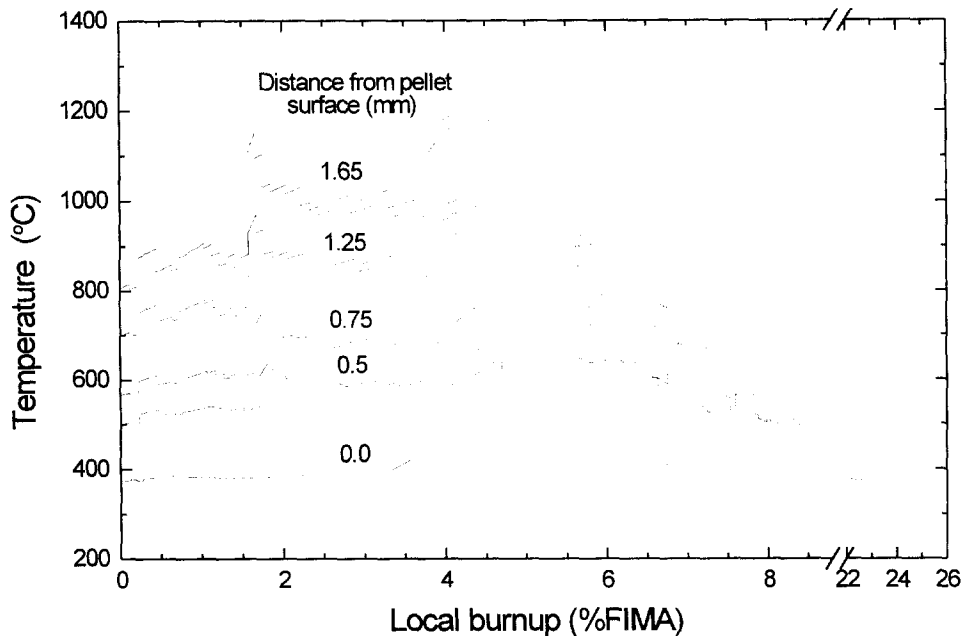


Fig. 2. Calculated temperature history at different radial local positions.

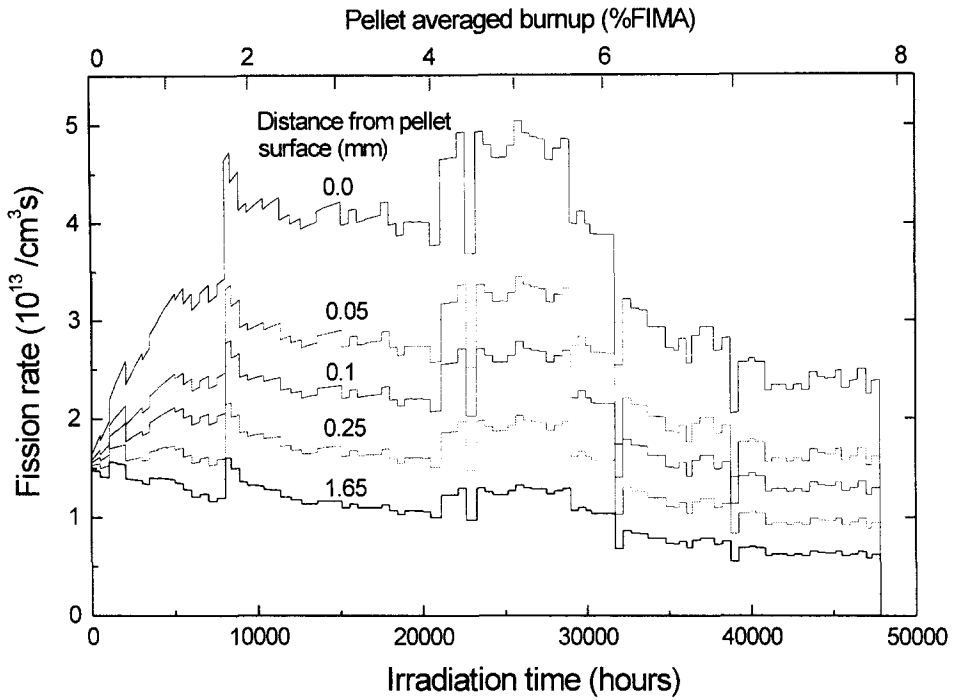


Fig. 3. Calculated fission rate at different radial local positions.

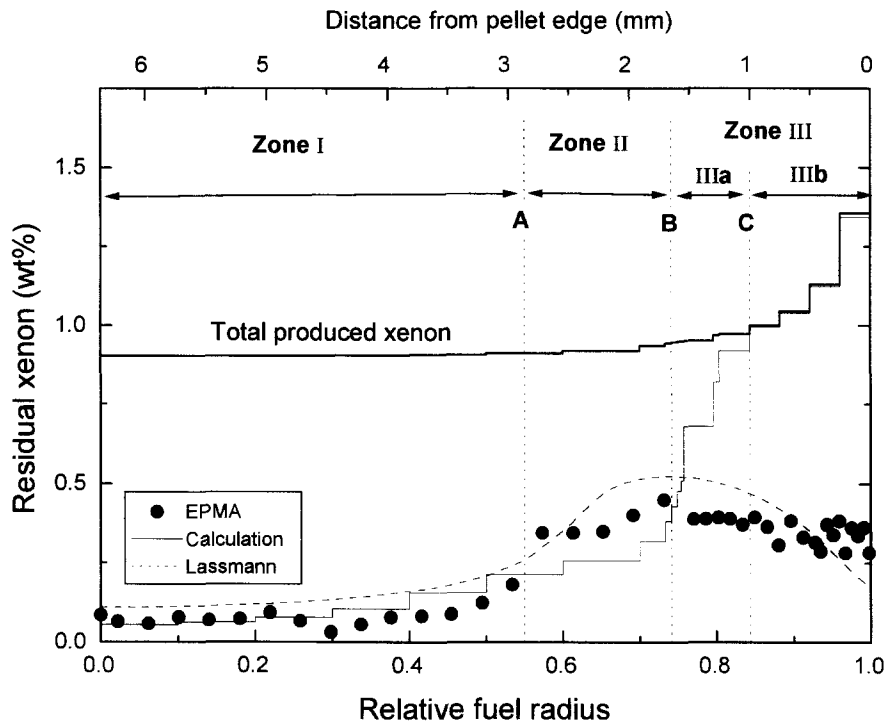


Fig. 4. Comparison of calculated retained gas and EPMA measurement as a function of fuel radius.

as zones I, II and III. The calculational results are compatible with the EPMA results within the two zones I and II only. Zone I extends from the center ( $r/r_0 = 0$ ) to  $r/r_0 \approx 0.55$  and is defined by very low EPMA signals which indicates thermally activated gas release due to the experienced high temperatures near the pellet center (see Figs. 1 and 2). The remaining fuel ( $0.55r_0$  to  $r_0$ ) shows essentially a plateau of EPMA signals. We divided this plateau into two zones (II and III). In zone II positioned between  $\approx 0.55r_0$  and  $0.73r_0$ , i.e. between 2.87 and 1.65 mm from the surface, no grain subdivision was observed indicating that the gas release was also thermally activated. On the other hand, the zone III is defined by the extent of the rim structure as observed by SEM [9]: grain subdivision was found extending from the pellet rim ( $r = 1.0r_0$ ) to a depth of 1.65 mm ( $r = 0.73r_0$ ).

Within the zone III, the EPMA signal tends to decrease towards the pellet surface, which is the typical observation for fuel with rim structure formation. The measured fraction of retained gas varies between 0.25 and 0.3 wt%. This is consistent with the value of 0.22 wt% for the fully developed high burnup structure (HBS) defined by Lassmann et al. [5], which was obtained from an extensive database of EPMA results at the Institute for Transuranium Elements. This agreement might be taken as indicating that zone III is totally restructured. The SEM observation [9] revealed that a large fraction of zone III is found to be restructured up to 1 mm from the surface (point C in Fig.

4). This zone is defined as IIIb. The EIMUS code calculations show low irradiation temperatures and absence of thermal fission gas release in zone IIIb. Complete retention of the gas is expected. Further SEM investigations were made to identify the degree of restructuring from 1 mm towards the center of the pellet. The fraction of restructured grains is decreasing and at the front point B (at 1.65 mm depth, or  $r/r_0 = 0.73$ ), restructuring is found only at few local sites such as pore surfaces. The zone between 1 mm and 1.65 mm depth (point B) is defined as zone IIIa. Fig. 1 shows parts of the optical ceramography of the investigated cross section at different radial locations. Fig. 1a and b show locations within zone I, revealing metallic precipitates, and indication of columnar and equiaxed grain growth caused by high temperature. Fig. 1c shows the location around the point B, the boundary of zones II and IIIa, indicating a transition of porosity growth. Clearly, thermal restructuring occurred also in zone II due to the experienced high temperatures.

Knowing the history of gas release at point B is of interest in obtaining a better understanding of the restructuring mechanism. The radial location of this point was irradiated at near to the (assumed) threshold temperature of fission gas release. The present best estimation by the EIMUS code indicates that position B experienced high temperatures and that significant gas release occurred between 3.96% FIMA local (4.29% FIMA pellet average) and around 5.6% FIMA, as shown in Figs. 2 and 5. This

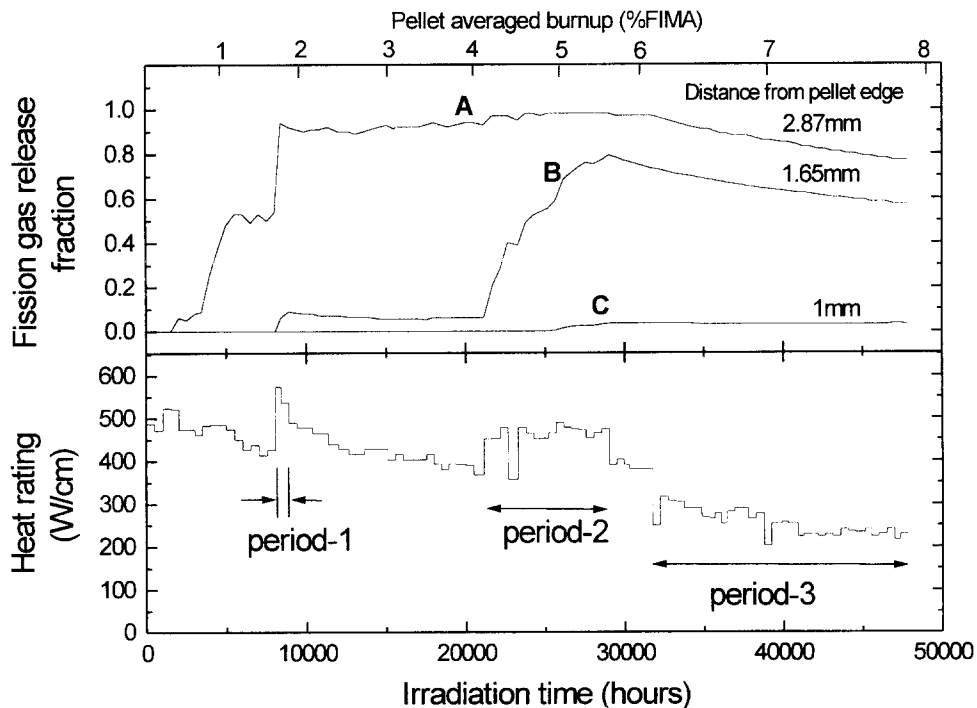


Fig. 5. History of rod averaged linear heat rating and calculated local fission gas release at three different radial positions corresponding to point A, B and C in Fig. 4.

analytical result could be supported by the observed boundary of porosity formation indicated in Fig. 1c. Around the position B, the amount of retained gas is likely to be reduced by thermally activated release during this burnup period and the reduced gas inventory may be associated with the cessation of the observed grain subdivision.

## 5. Discussion

The whole cross section of the analyzed fuel exceeded the often quoted threshold value for rim structure formation of 7% FIMA. No rim structure was observed in zones I and II, i.e. from  $r/r_0 \approx 0.72$  to the centre of the pellet. This was previously suggested to be due to the high temperature and to thermally activated mechanisms [3]. The aim of the revised calculation in the present paper was to improve the calculation of the temperature history and to obtain the *local* fission gas release values as accurately as possible. Although the accuracy may be further improved in the future, we present Fig. 5 which shows calculated local histories of gas release together with the power history. The curves correspond to the radial positions A, B and C shown in Fig. 4. The local burnup and the pellet averaged burnup are rather similar at these positions. For example, the final burnup of position C is 7.6% FIMA, which is slightly less than the 7.9% of the pellet average. The calculations suggest that zone II lost fission gas during period 2 with the highest temperatures due to the combined effects of high power and degradation of the thermal conductivity (see also Fig. 2). Period 2 lasted for 7000 h (9 months) and period 3 lasted for 15 000 h (1.7 years). At position B the gas inventory recovered during the long term period 3. The decrease of the gas inventory and the recovery of irradiation damage might affect the restructuring process in zone IIIa.

Based on these analytical results, we conclude that the zone IIIa is a transition zone which experienced both processes of thermal activation and of grain sub-division. Thermally activated fission gas release was predicted to start at 1.25 mm depth and to be  $\approx 60\%$  at the restructuring front (1.65 mm depth or  $r/r_0 = 0.73$ ). The observed reduction of the EPMA signal would thus be a result of both thermal and athermal mechanisms. The mechanism for the observed disappearance of the grain sub-division near the point B can be considered based on these analytical results. Concerning the irradiation damage, the temperature in period 2 is not high enough to annihilate accumulated dislocations, whereas point defects will be annihilated during this period. However, point defects are continuously generated and saturation is achieved rather soon also during period 3. Therefore, the irradiation damage and the stored energy by damage accumulation might not have been affected by period 2 and point defect accumulation alone will not be the main mechanism of the grain sub-division. Equally, the lattice distortions by incorporating rare

earth fission products will not have been affected by the high temperatures during period 2. On the other hand, the gas inventory was significantly affected by the temperature history and it was only partially restored during period 3. This gas behavior may thus explain the population profile of the grain sub-division in zone IIIa. The disappearance of the grain sub-division near the point B could therefore be due to loss of the fission gas.

The size distribution of the new subgrains observed by SEM is almost identical between the surface and the inner front at point B [9]. A similar constant subgrain size ( $\approx 0.3 \mu\text{m}$ ) has also been seen in power reactor fuel at high burnup [19]. The local temperatures, shown in Fig. 2, differ relatively widely in this zone, ranging from 400 to 800°C during period 3. This confirms that the process to form subdivided grains of  $\approx 0.3 \mu\text{m}$  diameter is not controlled by the temperature in this range. On the other hand, new grains with a smaller averaged diameter of 0.16  $\mu\text{m}$  were found near the pellet edge in the fully restructured zone where a bimodal sub-grain size distribution (peaked at 0.16 and 0.3  $\mu\text{m}$ ) was observed in TEM [9]. The fission rate was high at the fuel pellet surface as shown in Fig. 3 and so is the burnup. It is at present difficult to attribute one of these parameters to the observed smaller grains of  $\approx 0.16 \mu\text{m}$ .

The dotted line in Fig. 4 shows a model calculation by Lassmann et al. [5], which describes the xenon depletion observed by EPMA. It reproduces the general trend of the data over the radial zones. This model aims to give a quantitative description of the restructuring and it may describe the gas localization process, which corresponds to the number and size distribution of bubbles and/or planar defects. On the other hand the bubble swelling due to the restructuring ceases around the point B in Fig. 4. This observation is the main concern of the present paper. The calculations by the code suggest that the fuel temperature and gas release are the most probable cause of the end of the transition zone IIIa, where the restructuring was ceasing and terminated. However, further experimental data, such as from an ongoing tailored irradiation [6], are necessary to identify details of the governing processes and determine the mechanism.

## 6. Summary and conclusions

A section of a high burnup  $\text{UO}_2$  fuel rod with a pellet average burnup of 7.9% FIMA was carefully re-analyzed by combining neutronic and thermal codes and the results were compared with newly obtained microstructural observations by TEM and SEM [9]. The calculations yielded the time dependence of fission rate, temperature and fission gas release at different pellet radial positions as a function of local burnup. The particular fuel had been selected because it experienced a period of 300 days of increased temperatures in the middle of its irradiation time of 5.5 years, thus affecting e.g. the local fission gas content.

The electron microscope analysis showed, as described in the companion paper [9], a fully restructured rim region and extension of grain subdivision into the fuel to a depth of 1.65 mm ( $r/r_0 = 0.73$ ). The calculations yielded temperatures of about 1200°C and high gas release at this restructuring front during the period of increased temperature. Unfortunately, a similar extensive SEM/TEM study for a fuel of the same burnup but without the high temperature period is not available for comparison. Nevertheless, some interesting conclusions on the parameters affecting grain subdivision and polygonization in  $\text{UO}_2$  seem possible.

(1) The calculation results suggest strongly confirm that fuel restructuring does not occur where extensive thermal gas release is experienced, though the whole analyzed cross section exceeded 7% FIMA which is thought to be the threshold of the restructuring. The code calculations showed that thermal gas release occurred at the restructuring front at half the final burnup and that a significant part of the generated gas was lost during the high power period.

(2) The grain size distribution, centered around a diameter of 0.30  $\mu\text{m}$ , did not vary significantly with radial position between 50 and 1650  $\mu\text{m}$  depth. Calculations show that neither local temperature (range 400 to 1100°C), final burnup (range 7.2 to > 20% FIMA) nor fission rate (range 1 to  $5 \times 10^{13}$  f/cm<sup>3</sup> s) had a significant effect on the subgrain size. This suggests that the restructuring occurred once and thereafter the morphology was stable during the following burnup increments. Also, the mechanism to form the subgrains of  $\approx 0.30 \mu\text{m}$  is also likely to be the same, between the pellet surface and the depth of 1.65 mm (note, however, that TEM revealed some smaller grains of  $\approx 0.16 \mu\text{m}$  diam. in the fully restructured rim zone, a so-far unexplained observation).

(3) The effect of the high temperature phase on radiation damage is more complex. While point defects will be annihilated by recombination and/or migration to sinks, extended defects, in particular dislocation networks, are less affected by the high temperature period and will largely have survived this period. The same is true for distortion of the  $\text{UO}_2$  lattice by incorporated rare earth fission products. Therefore, even though a high temperature period was experienced, the continued additional irradiation period at reduced temperatures, from 5.2 to 7.2% FIMA, could nevertheless trigger the restructuring at the normal threshold. The investigation of this particular fuel indicates, however, that restructuring stops at the radial location at which a significant amount of fission gas is released during an intermediate burnup stage.

For future research to better define these parameters, the development and the thermal stability of tangled dislocations, dislocation networks and their interplay with fission gas bubbles and solid fission product precipitates as

well as the effect of soluble fission products in the  $\text{UO}_2$  matrix should be studied.

### Acknowledgements

The authors like to thank J. Spino for many helpful discussions. They would also like to thank P. Knudsen and his colleagues for reviewing and providing the power history of the rod AF 21-2 to improve the accuracy of the analysis, and V.V. Rondinella for the help in revising the manuscript.

### References

- [1] Hj. Matzke, J. Nucl. Mater. 189 (1992) 141.
- [2] T. Kameyama, T. Matsumura, M. Kinoshita, Nucl. Technol. 106 (1994) 334.
- [3] C.T. Walker, T. Kameyama, S. Kitajima, M. Kinoshita, J. Nucl. Mater. 188 (1992) 73.
- [4] P. Knudsen, C. Bagger, M. Mogensen, H. Toftegaard, IAEA Technical Committee Meeting on Fission Gas Release and Fuel Rod Chemistry Related to Extended Burnup, Apr. 28–May 1, 1992, Pembroke, Ontario, Canada.
- [5] K. Lassmann, C.T. Walker, J. van de Laar, F. Lindström, J. Nucl. Mater. 226 (1995) 1.
- [6] M. Kinoshita, S. Kitajima, T. Kameyama, T. Matsumura, E. Kolstad, Hj. Matzke, ANS Int. Topical Meeting on LWR Fuel Performance: Going beyond Current Burnup Limits, Portland, Mar. 2–6, 1997, p. 530.
- [7] M.E. Cunningham, M.D. Freshley, D.D. Lanning, J. Nucl. Mater. 188 (1992) 19.
- [8] K. Une, K. Nogita, S. Kashibe, M. Imamura, J. Nucl. Mater. 188 (1992) 65.
- [9] I.L.F. Ray, Hj. Matzke, H.A. Thiele, M. Kinoshita, J. Nucl. Mater. 245 (1997) 115.
- [10] Hj. Matzke, in: R. Agarwala (Ed.), Diffusion Processes in Nuclear Materials, North Holland, Elsevier, Amsterdam, 1992, p. 9.
- [11] Hj. Matzke, A. Turos, G. Linker, Nucl. Instrum. Meth. B91 (1994) 294.
- [12] Hj. Matzke, P.G. Lucuta, R.A. Verrall, J. Nucl. Mater., in preparation.
- [13] M. Kinoshita, J. Nucl. Sci. Technol. 30 (1993) 1.
- [14] S. Kitajima, M. Kinoshita, IAEA Technical Committee Meeting on Fission Gas Release and Fuel Rod Chemistry Related to Extended Burnup, Apr. 28–May 1, 1992, Pembroke, Ontario, Canada.
- [15] P.G. Lucuta, Hj. Matzke, I. Hastings, J. Nucl. Mater. 232 (1996) 166.
- [16] P.G. Lucuta, R.A. Verrall, Hj. Matzke, B.J. Palmer, J. Nucl. Mater. 178 (1991) 48.
- [17] S. Ishimoto, M. Hirai, K. Ito, Y. Korei, J. Nucl. Sci. Technol. 31 (1994) 796.
- [18] C. Bagger, M. Mogensen, C.T. Walker, J. Nucl. Mater. 211 (1994) 11.
- [19] J. Spino, K. Vennix, M. Coquerelle, J. Nucl. Mater. 231 (1996) 179.